The 2014 World Congress on
Advances in Civil, Environmental, and Materials Research (ACEM14)
Busan, Korea, August 24-28, 2014

Photodegradation of pharmaceuticals by $BiOCl_xI_y$ under simulated solar and visible irradiation

Xiaoning Wang[1)], Hongjing Li[2)], *Wenbo Dong[3)]

[1), 2) 3)] *Shanghai Key Laboratory of Atmospheric Particle Pollution and Prevention, Department of Environmental Science & Engineering, Fudan University, Shanghai, 200433, China*
[3)] wbdong@fudan.edu.cn

ABSTRACT

Photodegradation of hydroxyphenylacetic acid (p-HPA) and acetaminophen (ACTP) was investigated under simulated solar and visible irradiation using $BiOCl_xI_y$. The combination of BiOCl and BiOI has largely improved the photocatalytic activity both under solar and visible light, and $BiOCl_{0.75}I_{0.25}$ was obtained as the optimal catalyst. Under simulated solar light, complete degradation of p-HPA was achieved after 180min in the presence of 0.6 g/L $BiOCl_{0.75}I_{0.25}$. While ACTP was degraded about 80% in the same condition because ACTP had a much less adsorption by $BiOCl_{0.75}I_{0.25}$. Under simulated visible light, the degradation efficiency of both p-HPA and ACTP decreased. In particular, BiOCl exhibited no photodegradation of p-HPA and ACTP in visible light. Experimental results demonstrated that photocatalytic reactions of p-HPA and ACTP followed pseudo-first-order kinetics.

1, INTRODUCTION

In the recent decades, pharmaceuticals and personal care products (PPCPs) in the environment have emerged as a new environmental concern. Pharmaceuticals were widely detected in ground water, surface water, even in drinking water. These kinds of pollutant include analgesics, anti-inflammatory drugs, antibiotics, lipid regulators, psychiatric drugs, and β-blockers, detected in concentrations ranging from ng/L to a few μg/L in wastewater influent (Jelic 2011, Lin 2008). Due to its trace concentration in water and reluctance to biological degradation for some kinds of pharmaceuticals, sewage treatment plants (STPs) cannot remove all the pollutant completely. Levels of many pharmaceutically active compounds (PhACs) are barely reduced and can be detected in wastewater-treatment plant (WWTP) effluents.

[1)] Graduate student
[2)] Doctor
[3)] Professor

Hydroxyphenylacetic acid (p-HPA) (Fig, 1a) is one kind of pharmaceutical intermediates, widely used in the synthesization of medicine and pesticide. Furthermore, p-HPA was commonly detected in olive oil wastewater (Sanchez et al). Acetaminophen (ACTP) (Fig, 1b) is extensively used as an analgesic and antipyretic drug all over the world, ranked as one of the top 25 prescriptions in the UK (Jones 2012). After released to water, these two pollutants cannot be photodegraded under sunlight.

So degradation of pharmaceutical wastewater by advanced oxidation processes (AOPs) such as UV (Kawabata 2012), Ozone/UV (Miranda 2002) and Fe^{2+}/ H_2O_2 (Luna 2014) have been came into use for many years. In the same time, photocatalytic degradation has drawn more and more attention. Semiconductive catalyst such as TiO_2 (Moctezuma 2012) is widely used because of its nontoxicity and high efficiency of photo degradation. However, its large band gap (3.2ev) determines that it only can be irradiated under UV-light, so semiconductor photocatalyst driven by visible light has become the world hot topic. In this group, Bi-based compounds such as Bi_2O_3 (Chai 2009), $Bi_2O_2CO_3$ (Zhang 2014), Bi_2S_3 (Jiang 2014) and BiOX (X=Cl, Br, I) (Zhang 2008) receive wide attention due to their characteristic hierarchical structures and high photocatalytic activities. In particular, BiOX has been synthesized by sol-gel (Wang 2014), solvethermal (Xiao 2012), precipitation (Dong 2012) and reverse microemulsions methods, showing excellent performance in purifying various pollutants in wastewater.

BiOCl is one kind of promising materials owing to its high separation of photo-induced electron-hole pairs (Wu 2011). Under visible light, BiOI showed the best degradation efficiency due to its narrow band gap (1.76ev) (Hao 2012 and Qin 2013). So combination of BiOCl and BiOI was widely studied in recent years (Wang 2007). Often by solvethermal method, flower-like hierarchical BiOCl/BiOI could be synthesized successfully, but high temperature and long reaction time were required. While, precipitation methods could be conducted in relatively low temperature and ambient pressure. By this method, hierarchical porous BiOI/BiOCl composites have synthesized in aqueous solution by Dong et al, showing great photocatalytic degradation under visible light. In order to improve the surface areas and decrease the particle size of catalysts, solvent would play important roles in the synthesization process.

In this article, $BiOCl_xI_y$ composite materials have been synthesized in Ethylene glycol (EG)-water (H_2O) solvent by precipitation methods. The synthesized solids were characterized by X-ray diffraction (XRD) and field emission scanning electron microscopy (FESEM). Adsorption and photocdegradation of p-HPA and ACTP by these catalysts have been investigated under simulated solar light and visible light. Optimal $BiOCl_xI_y$ has been obtained by adjusting the different molar ratio of chlorine and iodine.

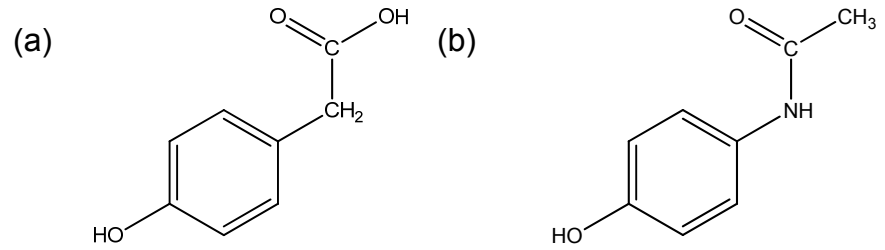

Fig.1. Structure of hydroxyphenylacetic acid (p-HPA) (a), acetaminophen (ACTP) (b)

2, EXPERIMENTAL

2.1, Synthesis of BiOI/BiOCl composites

All the reagents are analytical grade and used without further purification. Firstly, 12 mM $Bi(NO_3)\cdot 5H_2O$ was prepared in 24mL EG and kept stirring at 80℃ for 30 min. Then, KCl and KI with different molar ratio (1:0, 0.75:0.25, 0.5:0.5, 0.2:0.8 and 0:1) was dissolved in 96mL deionized water, keeping their total molar amount equal to $Bi(NO_3)\cdot 5H_2O$. The aqueous solution was added into the previous EG solution dropwise and the pH of this mixture was adjusted to 9.0 with $NH_3\cdot H_2O$. Afterwards, the solution remained stirring at 80℃ for 3h. Finally, the mixture was collected by centrifugation, washed several times with deionized water and ethanol, dried at 60℃. Then the samples were calcined at 200℃ for 2 h to remove the residual carbon.

2.2, Characterization

The crystal phase structure was characterized by X-ray diffraction (XRD, Bruker D8 Advance) using Cu Kα radiation (40kV and 40mA) as X-ray source (λ= 0.154056 nm) with a 2θ scope of 10–90° . The morphology of the photocatalyst was observed through field emission scanning electron microscopy (FESEM, Ultra 55, Germany).

2.3, Analytical methods

The concentration of p-HPA and ACTP in the reaction media was measured by HPLC (U-3000, USA) , using a XDB-C18 reverse phase column (5 m, 4.6 mm × 150 mm) with UV detector (λ= 274 nm, λ=244nm). For p-HPA, Methanol (HPLC-grade), water (HPLC-grade, pH=3.06, adjusted by acetic acid) were used as mobile phase (50:50, v/v), at a flow rate of 0.8 mL min^{-1}. For ACTP, Methanol (HPLC-grade) and water (HPLC-grade) were used as mobile phase (40:60, v/v), at a flow rate of 0.8 mL min^{-1}.

2.4, Photocatalytic experiments

The reaction was conducted in a photochemical reactor (XPA-VII, Nanjing Xujiang Machine electronic Plant, China), equipped with a 500 W Xe lamp combined with a 290

nm and 420 cut-off filter as simulated solar light and visible light source. 50 mL p-HPA and ACTP solution (20mg/L) was contained in quartz cuvette mixed with 0.03g catalyst. During reaction process, the mixture was under constant magnetic stirring. Before irradiation, the suspension kept stirring for one hour in the dark to reach the adsorption-desorption equilibrium. During the photocatalytic process, approximately 1.5 mL of the suspension was withdrawn and the catalysts were removed from the solution using a 0.22 μm filter.

3, RESULTS AND DISCUSSION

3.1. Phase structure

Fig.2 shows the XRD patterns of the as-prepared $BiOI_xCl_y$ samples. All the samples can be indexed to tetragonal phase BiOCl (JCPDS card NO. 06-0249) or tetragonal phase BiOI (JCPDS card NO. 73-2062), and no other impure peaks can be observed. With the introduction of iodine molar ratio from 0 to 1.0, all diffraction peaks gradually shift to lower angles (Fig.2b). Bragg equation was shown in Equation 1, from which can be seen that with the increasing of d, θ would decrease. Cl^- has a smaller ionic radius than I^- (1.81 vs 2.16), so conclusion can be made that solid solutions have been formed in $BiOI_xCl_y$ composite (Dong 2012). Also it can be seen that, peaks of the composite solid were broader and weaker than pure BiOCl and BiOI, implying lower crystallinity. Heterojunction would lead to lattice defects in these composite samples.

$$2d\sin\theta = n\lambda \ (n=1, 2, 3\ldots, \lambda = 0.154056 \text{ nm}) \quad (1)$$

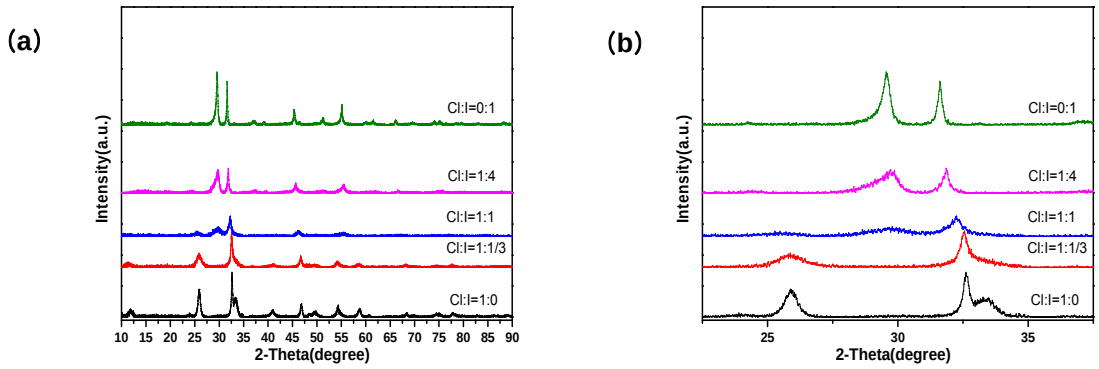

Fig.2. XRD patterns of the as-prepared $BiOCl_xI_y$ samples (a) and enlarged view of the diffraction region from 22.5 to 37.5° (b)

3.2 Morphology

The FESEM images of $BiOCl_{0.75}I_{0.25}$ were shown in Fig.3a. It can be seen that all the samples exhibited irregular flower-like hierarchical structures of 200-400 nm in size. Other $BiOCl_xI_y$ showed the similar structure consisted of nanosheets. Won et al have synthesized the similar $BiOCl_xI_y$ microspheres of 1–3 μm in size by solvethermal method, and Xiao et al synthesized $BiOCl_xI_y$ microspheres with diameters of approximately 2–4 μm. Flower-like $BiOCl_xI_y$ also has been synthesized with a size of 3-5μm via precipitation method in aqueous solution by Dong et al. While also by this method, in mixed solvent, smaller particle size solids were formed in this article. When $Bi(NO_3)\cdot 5H_2O$ was dissolved in EG firstly, EG is viscous enough the slowdown the speed of nucleation compared with the direct hydrolysis in water. Under continuous stirring, small-sized $BiOCl_xI_y$ particle nanosheets were formed at the initial stage, and at later stages, these sheets tended to aggregate into larger particles. Small particle sizes will lead to large surface area and high surface-to-volume ratio, increasing the adsorption of micro pollutant in water. The different color of $BiOCl_xI_y$ was shown in Fig.3b, changing from white to brick red with the ratio of iodine increasing.

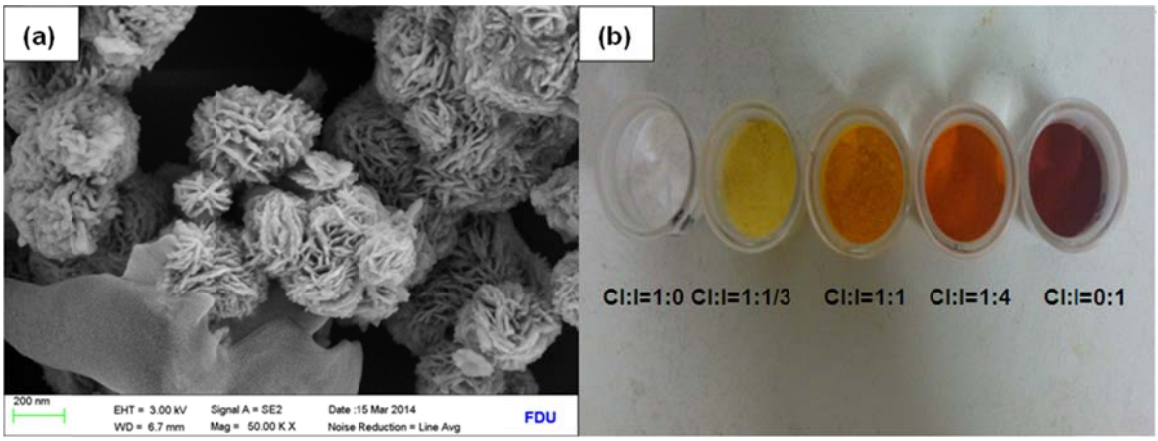

Fig.3. FESEM images of $BiOCl_{0.75}I_{0.25}$ (a) and color of the as-prepared $BiOCl_XI_y$ (x: y=1:0, 1:1/3, 1:1, 1:4, 0:1) solids (b)

3.3 Simulated solar light photocatalytic activity for removal of p-HPA and ACTP

The photodegradation of p-HPA and ACTP over the as-prepared samples under simulated solar light were displayed in Fig.4a and 4c. No degradation could be observed in the absence of any catalyst both for p-HPA and ACTP. Under dark condition for 1h, $BiOCl_XI_y$ showed great adsorption of p-HPA, while poor adsorption of ACTP. The adsorption efficiency of p-HPA by $BiOCl_XI_y$ ranked as x: y=1:1/3 (43%)>1:1 (31%)>1:0 (29%)>1:4 (24%)>0:1 (14%). Respectively, pure BiOCl displayed more adsorptional

ability than BiOI of p-HPA. With the introducing of iodine to BiOCl, composite samples $BiOCl_{0.75}I_{0.25}$ and $BiOCl_{0.5}I_{0.5}$ enhanced the adsorption performance. While with iodine further increasing, the adsorption of $BiOCl_{0.2}I_{0.8}$ decreased ascribing to the relatively poor adsorption of BiOI. While for ACTP, both pure sample and composite materials, no obvious adsorption could be detected. Great adsorption could supply more active sites, accelerating photocatalytic process.

Under simulated solar irradiation, degradation of p-HPA over $BiOCl_XI_y$ ranked as x: y=1:1/3 (100%)>1:0 (89%)>1:1 (82%)>1:4 (67%)>0:1 (43%). Pure BiOCl possessed greater photodegradation activity than BiOI, in consistent with the adsorption ability talked above. Upon the introducing of iodine, removal of p-HPA over catalyst $BiOCl_{0.75}I_{0.25}$ was dramatically enhanced. While further increasing the molar ratio of iodine, photodegradation abilities have decreased, due to the relative poor photocatalytic ability of BiOI. Xiao et al have demonstrated that composite materials with different conduction band (CB) and valence band (VB) can reduce the combination of photo induced electrons and holes. Similar mechanism also can be explained in this article. However, the degradation of ACTP showed different results. Under simulated solar irradiation, BiOI possessed greater photocatalytic properties than BiOCl. Photodegradation efficiency of ACTP with $BiOCl_XI_y$ was in the order of x: y=1:1/3 (81%)>1:4 (65%)>1:1 (62%)>0:1 (52%)>1:0 (34%). In general, ACTP have got poorer degradation than p-HPA, resulting from its weak adsorption. The results have shown that catalyst $BiOCl_XI_y$ possessed high solar light driven photocatalytic properties. In particular, $BiCl_{0.75}I_{0.25}$ obtained the greatest ability both for p-HPA and ACTP.

The reaction kinetics of p-HPA and ACTP for the as-synthesized composites followed pseudo first-order kinetics (R^2>0.9), as shown in Fig.4b and 4d.The equation (2) was used:

$$-\ln\left(\frac{Ct}{C0}\right) = k_{app}t \qquad (2)$$

where C_0 and C_t are the reactant concentrations at times t = 0 and t = t, respectively, and k_{app} (min^{-1}) is the apparent reaction rate constant determined by plotting $\ln(C_0/C_t)$ vs. the reaction time (t) (Xiao 2012). The specific k_{app} would be shown in Fig.6.

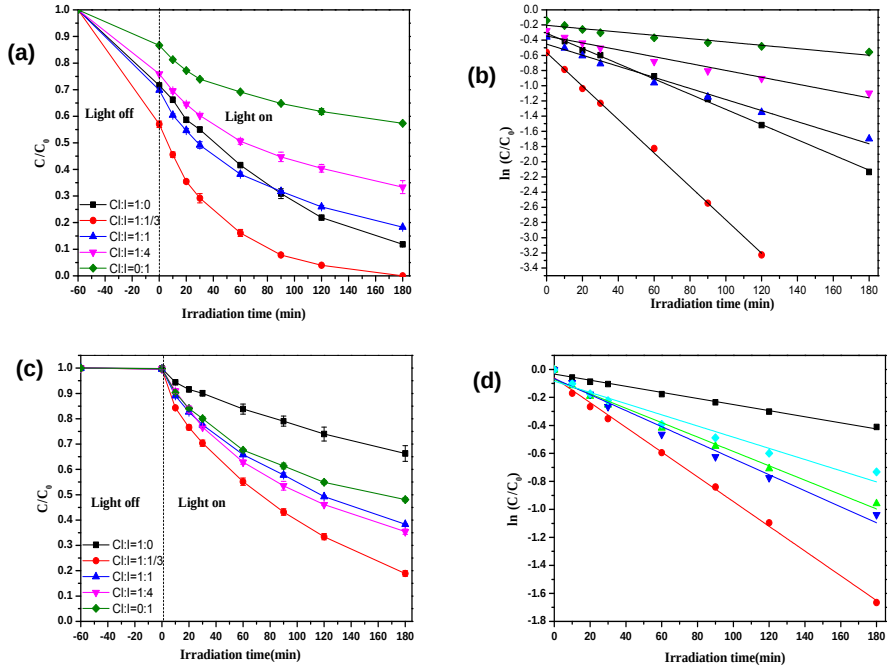

Fig.4. Photocatalytic activity of $BiOCl_XI_y$ for removal of p-HPA (a) and ACTP (b) under simulated solar light, pseudo-first-order kinetics of the photodegradation of p-HPA (c) and ACTP (d)

3.4 Simulated visible light photocatalytic activity for removal of p-HPA and ACTP

Fig.5a, c represented the degradation of p-HPA and ACTP under simulated visible light. Under visible light (λ>420nm), BiOCl displayed poor photodegradation both for p-HPA and ACTP, ascribing to its large band gap (3.2 ev), only could be irradiated under UV-light (Qin 2013). For p-HPA, adsorption ability of $BiOCl_XI_y$ stayed the same as discussed in Fig.4. While photodegradation efficiency of composite $BiOCl_XI_y$ ranked as x: y=1:1/3 (73%)>1:1 (68%)>1:4 (57%)>0:1(36%) >1:0 (30%), including the adsorption portion. This result kept the similar results compared with simulated solar light except for BiOCl. So BiOCl possessed high solar driven photocatalytic properties and poor visible driven photocatalytic ability. This phenomenon played the same in the degradation of ACTP. In the photocatalysis of ACTP, $BiOCl_XI_y$ (x:y=1:1/3 1:1 1:4 0:1) exhibited the similar results, ranking as x: y= 1:1 (47%)=1:4 (47%)=0:1 (47%)>1:1/3 (38%)>1:0 (0%). As shown in Fig.5b, d, reaction kinetics of p-HPA and ACTP for the as-synthesized composites well fitted with pseudo first-order kinetics (R^2>0.9). The specific k_{app} would also be shown in Fig.6.

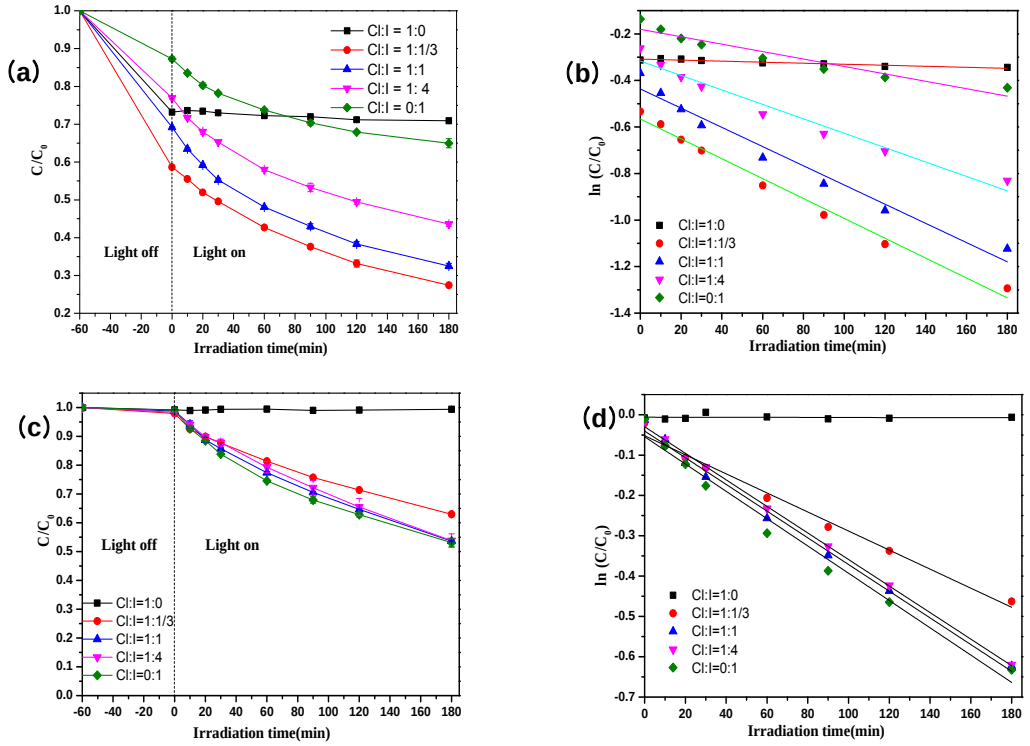

Fig.5. Photocatalytic activity of $BiOCl_XI_y$ for removal of p-HPA (a) and ACTP (b) under simulated visible light, pseudo-first-order kinetics of the photodegradation of p-HPA (c) and ACTP (d)

3.5 Compare of k_{app} under different light

As discussed in Fig.4 and Fig.5, photodegradation kinetics of p-HPA and ACTP for the as-synthesized composites well fitted with pseudo first-order kinetics (R^2>0.9) both under simulated solar and visible light. It can be seen that degradation of both p-HPA and ACTP possessed higher k_{app} under solar light than visible light, especially for BiOCl (Fig.6). This meant that light with a wavelength between 290nm and 420nm was very important for the degradation of pollutant by $BiOCl_XI_y$. Under solar irradiation, $BiOCl_{0.75}I_{0.25}$ exhibited predominant photocatalytic activities both for p-HPA and ACTP, implying one kind of potential catalyst in purifying pollutant in the future.

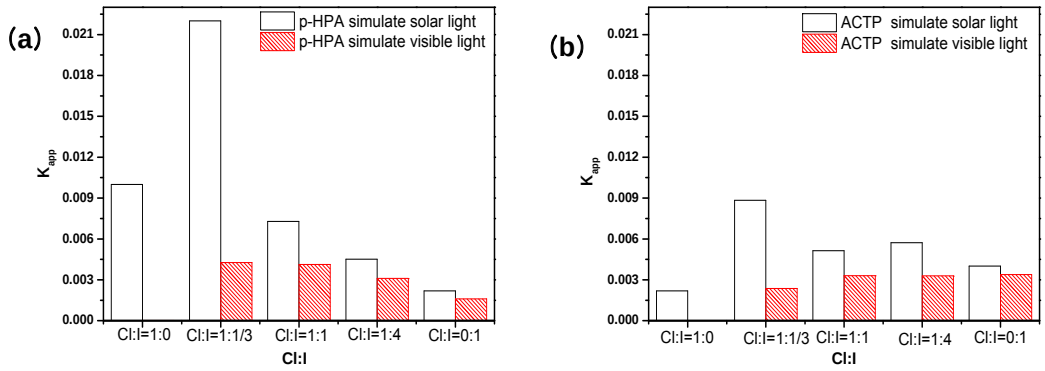

Fig.6 k_{app} of pseudo first-order kinetics for photodegradation of p-HPA (a) and ACTP (b) under simulated solar and visible light

4, CONCLUSION

$BiOCl_xI_y$ was synthesized in EG-H_2O mixed solvent by precipitation method successfully. The characters of $BiOCl_xI_y$ showed that solid solution was formed in these composite materials from XRD. The synthesized solid exhibited in microsphere, possessing small particle size from FESEM. $BiOCl_xI_y$ was used to photo degrade p-HPA and ACTP under simulated solar and visible irradiation. Photodegradation and adsorption was affected by the molar ratio between chlorine and iodine. Under solar light, $BiOCl_{0.75}I_{0.25}$ showed predominant catalytic efficiency both for p-HPA and ACTP. While under visible light, photodegradation efficiency decreased, especially for BiOCl, as displayed in the comparation of k_{app}. $BiOCl_xI_y$ showed great potential practical application in removing pollutant from water in the future.

5, REFERENCES

Chai S.Y. and Kim Y.J. (2009), “Heterojunctioned $BiOCl/Bi_2O_3$, a new visible light photocatalyst”, J Catal, 262, 144–149.

Dong F. and Sun Y. (2012), “Room temperature synthesis and highly enhanced visible light photocatalytic activity of porous BiOI/BiOCl composites nanoplates microflowers”, *J Hazard Mater,* 219–220, 26–34.

Hao R. and Xiao X. (2012), “Efficient adsorption and visible-light photocatalytic degradation of tetracycline hydrochloride using mesoporous BiOI microspheres”, *J Hazard Mater*, 209–210, 137–145.

Jelic A. and Gros M. (2011), “Occurrence, partition and removal of pharmaceuticals in sewage water and sludge during wastewater treatment”, *water res.,* 45, 1165-1176.

Kawabata K. and Kawabata K. (2012), "Ultraviolet-photoproduct of acetaminophen: Structure determination and evaluation of ecotoxicological effect", *J Photoch Photobio A*, 249, 29– 35.

Lin A. Y. and Yu T. (2008), "Pharmaceutical contamination in residential, industrial, and agricultural waste streams: Risk to aqueous environments in Taiwan", *Chemosphere*, 74, 131–141.

Luna M. D. G. and Veciana M. L. (2014), "Factors that influence degradation of acetaminophen by Fenton processes", *J Taiwan Inst Chem E ,* 45, 565–570.

Jiang S.H. and Zhou K.Q. (2014), "In situ synthesis of hierarchical flower-like Bi_2S_3/BiOCl composite with enhanced visible light photocatalytic activity", *Appl Surf Sci*, 290, 313–319.

Miranda M. A. and Mar´ın M. L. (2002), "Pyrylium salt-photosensitized degradation of phenolic contaminants present in olive oil wastewater with solar light Part III. Tyrosol andp-hydroxyphenylacetic acid", *Appl Catal B—Environ,* 35, 167–174.

Moctezuma E. and Leyva E. (2012), "Photocatalytic degradation of paracetamol: Intermediates and total reaction mechanism", *J Hazard Mater,* 243, 130–138.

O.A.H. Jones and N. Voulvoulis. (2002), "Aquatic environmental assessment of the top 25 English prescription pharmaceuticals", *water res.*, 36, 5013–5022.

Qin X. and Cheng H. (2013), "Three dimensional BiOX (X=Cl, Br and I) hierarchical architectures: facile ionic liquid-assisted solvothermal synthesis and photocatalysis towards organic dye degradation", *Mater Lett*, 100, 285–288.

Sanchez I. and Stüber F. (2012), "Degradation of model olive mill contaminants of OMW catalysed by zero-valent iron enhanced with a chelant", *J Hazard Mater*, 199–200: 328–335.

Wang P. and Wu Y. L. (2014), "Preparation of carbon-supported Bi/Ti composites and its catalytic activity under solar irradiation", *Appl Surf Sci,* 292, 1077–1082.

Wang W. and Huang F. (2007), "xBiOI–(1-x)BiOCl as efficient visible-light-driven photocatalysts", *Scripta Mater*, 56, 669–672.

Won J. K. and Debabrata P. (2014), "Adsorption/photocatalytic activity and fundamental natures of BiOCl and $BiOCl_xI_{1-x}$ prepared in water and ethylene glycol environments,and Ag and Au-doping effects", *Appl Catal B—Environ,* 147, 711–725.

Wu S. and Wang C. (2011), "BiOCl nano/microstructures on substrates: Synthesis and photocatalytic properties", *Mater Lett*, 65, 1344–1347.

Xiao X. and Hao R. (2012), "One-pot solvothermal synthesis of three-dimensional (3D) BiOI/BiOCl composites with enhanced visible-light photocatalytic activities for the degradation of bisphenol-A", *J Hazard Mater,* 233–234, 122–130.

Zhang X.C. and Guo T.Y. (2014), "Facile composition-controlled preparation and photocatalytic application of BiOCl/$Bi_2O_2CO_3$ nanosheets", Appl Catal B—Environ, 150–151, 486–495.

The 2014 World Congress on
Advances in Civil, Environmental, and Materials Research (ACEM14)
Busan, Korea, August 24-28, 2014